Sheffield Hallam University

Complimentary Metal-Oxide-Semiconductor compatible deposition of nanoscale transition-metal nitride thin films for plasmonic applications

BOWER, Ryan, LOCH, Daniel <http://orcid.org/0000-0003-3252-0142>, WARE, Ecaterina, BERENOV, Andrey, ZOU, Bin, HOVSEPIAN, Papken, EHIASARIAN, Arutiun and PETROV, Peter

Available from Sheffield Hallam University Research Archive (SHURA) at:

https://shura.shu.ac.uk/27205/

This document is the Accepted Version [AM]

Citation:

BOWER, Ryan, LOCH, Daniel, WARE, Ecaterina, BERENOV, Andrey, ZOU, Bin, HOVSEPIAN, Papken, EHIASARIAN, Arutiun and PETROV, Peter (2020). Complimentary Metal-Oxide-Semiconductor compatible deposition of nanoscale transition-metal nitride thin films for plasmonic applications. ACS Applied Materials and Interfaces. [Article]

Copyright and re-use policy

See http://shura.shu.ac.uk/information.html

Sheffield Hallam University Research Archive
http://shura.shu.ac.uk

CMOS compatible deposition of nanoscale transition metal nitride thin films for plasmonic applications

Ryan Bower†, Daniel A. L. Loch‡, Ecaterina Ware†, Andrey Berenov†, Bin Zou†, Papken Eh. Hovsepian‡, Arutiun P. Ehiasarian‡, Peter K. Petrov†*

† Department of Materials, Imperial College London, Royal School of Mines, Exhibition Road, London, SW7 2AZ, UK

‡ National HIPIMS Technology Centre - UK, Materials and Engineering Research Institute, Sheffield Hallam University, Howard St., Sheffield, S1 1WB, UK

KEYWORDS: Transition metal nitride, multilayer structures, plasmonics, CMOS compatible, High Power Impulse Magnetron Sputtering

ABSTRACT: Transition metal nitrides have received significant interest for use within plasmonic and optoelectronic devices due to their tunability and environmental stability. However, deposition temperature remains a significant barrier to widespread adoption through the integration of transition metal nitrides as plasmonic materials within CMOS fabrication processes. Binary, ternary and layered plasmonic transition metal nitride thin films based on titanium and niobium nitride are deposited using High Power Impulse Magnetron Sputtering (HIPIMS) technology. The increased plasma densities achieved in the HIPIMS process allow thin films with high plasmonic quality to be deposited at CMOS compatible temperatures of less than 300°C. Thin films are deposited on a range of industrially relevant substrates and display tunable plasma frequencies in the ultraviolet to visible spectral ranges. Strain mediated tunability is discovered in layered films compared to ternary films. The thin film quality, combined with the scalability of the deposition process, indicates that HIPIMS deposition of nitride films is an industrially viable technique and can pave the way towards the fabrication of next-generation plasmonic and optoelectronic devices.

INTRODUCTION

Plasmonic materials have a wide range of applications, from energy storage and harvesting to biosensing and memory storage devices.[1–4] However, the archetypal plasmonic materials gold and silver are limited in their applicability, displaying poor thermal stability, limited spectral tunability, and incompatibility with standard CMOS fabrication processes.

Consequently, transition metal nitrides (TMNs), including titanium nitride and niobium nitride have been suggested as viable alternative plasmonic materials. In addition to superior mechanical and thermal properties compared to gold and silver,[5] TMNs also offer spectral tunability of the plasmonic response, with optical properties dependent on phase, stoichiometry and oxygen impurities.[6] Broadband spectral tunability is observed in ternary transition metal nitrides and is achieved by varying cation ratios.[7] Furthermore, TMNs such as titanium nitride are currently used within CMOS compatible fabrication processes as barrier layers and gate metals.[8–12] However, applications of TMNs are not yet optimised for optical behaviour and as such, the widespread use of TMNs within plasmonic and optoelectronic devices is limited.

A significant barrier to the application of transition metal nitrides as plasmonic materials within CMOS processes is the prohibitively high temperatures required for optimised thin film optical behaviour (>400°C).[13] This is an area of active research within the plasmonic community and significant strides are being taken to achieve low temperature and CMOS compatible deposition of high-quality TMNs. This has involved the deposition of nitride thin films using a variety of deposition techniques including pulsed laser deposition, DC and RF magnetron sputtering and plasma-enhanced atomic layer deposition.[14–16] Deposition by RF sputtering of plasmonic TiN was recently achieved at room temperature and short target-to-substrate distance of 5 cm allowing significant plasma density of the order of 10^{10} cm^{-3} and flux of nitrogen ions to reach to substrate.[14]

High Power Impulse Magnetron Sputtering (HIPIMS) can be used to deposit binary and ternary transition metal nitride thin films at CMOS compatible temperatures. HIPIMS utilises high instantaneous powers to produce plasma density of the order of 10^{13} cm^{-3} at the substrate which activates the deposition process by increasing the ionisation degree of the sputtered flux and the dissociation rate of the reactive gas ions. Del Giudice et al. have previously deposited micron thick TiNbN films using a hybrid HIPIMS and DC magnetron sputtering method at room temperature.[17] Ehiasarian et al. reported full morphological densification of TiN thin films[18] due to high

surface mobility and reactivity of the adatom flux and the promotion of (002) crystallographic texture which favours the incorporation of impurities such as oxygen as substitutions or interstitials into the growing crystal lattice of the films and reduces its segregation at grain boundaries.

Transition metal nitride thin films of the form $Ti_{(1-x)}Nb_xN_y$ were deposited on a range of industrially relevant substrates, including MgO, Si, and glass via confocal HIPIMS. The HIPIMS process enables high dissociation and ionisation during deposition which allows access to lower substrate temperatures of 300°C, compatible with CMOS fabrication flow. We report the structural properties of co-sputtered ternary transition metal nitrides with multi-layered binary nitrides, and correlate these with optical properties as measured by spectroscopic ellipsometry.

Results and discussion

Layered transition metal nitride structures consisting of alternating layers of binary TiN and NbN thin films were deposited on a range of industrially relevant substrates, including, MgO, Si, and glass via confocal HIPIMS at 300°C. Films were also deposited on steel, however, as this is not a substrate used in CMOS processes, all characterisation data for these films have been included in the Supporting information (S3,5) and will not be discussed in further detail here. The layered films have a total thickness of 100 nm and individual layer thicknesses of 5 nm and 10 nm. In addition CMOS compatible, binary and ternary transition metal thin films of the form $Ti_{(1-x)}Nb_xN_y$ were also deposited via HIPIMS. Films were 100nm thick and atomic force microscopy measurements of films deposited on Si substrates (S4) indicate that the root mean squared roughness is <1 nm.

Film composition for layered and ternary films was assessed via X-ray fluorescence (S2) for films on Si substrates. XRF data indicates cation stoichiometries of x = 0.52 within $Ti_{(1-x)}Nb_xN_y$ films. To further confirm film composition, EDS measurements were performed on co-sputtered $Ti_{(1-x)}Nb_xN_y$ films on Si substrates. Data were collected at 10 keV using an aperture of 60 microns and indicated that the elements present were niobium, titanium nitrogen and silicon (S2). Neglecting contributions from Si, the stoichiometry of the thin films was calculated to be $Ti_{0.51}Nb_{0.49}N_y$, in good agreement with the XRF data and close to the ratio expected from the deposition conditions. EDS analysis of both 10nm and 5nm layered superlattice films indicates film cation composition of $Ti_{0.52}Nb_{0.48}N$. XRD data indicates all films are polycrystalline with cubic rock-salt structure and dominant preferred orientation along the [111] and [002] directions (S3), in agreement with literature data for TiN, NbN and TiNbN films. As shown in Figure 1, ternary films deposited on MgO display a strong preferred orientation along the [002] direction with minimal contributions from the [111] and [220] orientations.

Figure 1b displays the variation in [002] peak position observed between binary and ternary films which corresponds to changes in the c-lattice parameter. For MgO substrates, the lattice parameters obtained for the binary thin films TiN and NbN are 4.24 Å and 4.44 Å respectively. Compared to the literature values of 4.26 Å and 4.39 Å, we see a good agreement with the TiN lattice and a slight difference for the NbN film. This difference can be accounted for by considering strain within the thin film and variations in nitrogen stoichiometry, which have been shown to lead to lattice parameters of up to 4.64 Å.[19] Additionally, it is possible that there is epitaxial alignment with the MgO substrate, promoted by the similarity in lattice spacing and the clean surface obtained after plasma cleaning. This is further supported by the preferred orientation observed in the [002] lattice direction.

The lattice parameter for ternary films as calculated directly from peak positions obtained from XRD diffraction measurements of TiNbN films on MgO is 4.33 Å. This is in close agreement with the predicted value for $Ti_{0.51}Nb_{0.49}N_y$ of 4.34 Å calculated from Vegard's law.

In contrast to the MgO substrates, films deposited on Si substrates (Figure 1c) and glass (S3) display preferred orientation in the [111] and [002] crystallographic directions. Peaks observed are broad, potentially indicative of small crystallite size or inhomogeneous strain within the films. Nevertheless, as shown in Figure 1d, the peak positions for [111] and [002] preferred orientations display a clear trend in lattice parameter, as would be expected with the change in cation identity.

In order to investigate the suitability of these films for plasmonic applications, the film's optical properties were assessed using spectroscopic ellipsometry. Figure 2 displays the optical properties of $Ti_{(1-x)}Nb_xN_y$ films deposited on Si, glass and MgO substrates at 300°C via HIPIMS. Ellipsometric parameters psi and delta were measured at three angles (65°, 70° and 75°) and fit to a Drude - Lorentz (DL) model containing up to two Lorentz oscillators in order to extract the real (ε') and imaginary (ε") dielectric permittivity for each film. A summary of all DL fitting parameters can be found in S5.a. As can be seen from the real permittivity plots, all films display metallic optical behaviour above 320nm and optical properties comparable to literature values for TiN, NbN and TiNbN. [2,17,20–22]

The binary and ternary films display tuneable optical properties, in addition to highly metallic plasmonic behaviour. This is evident when considering the screened plasma energy, corresponding to the wavelength at which ε' = 0 or the epsilon-near-zero (ENZ) point. For $Ti_{(1-x)}Nb_xN_y$ films this is shown to be tunable over the range 320 – 490nm. This tunability arises due to variations in charge carrier concentration with cation identity and stoichiometry.

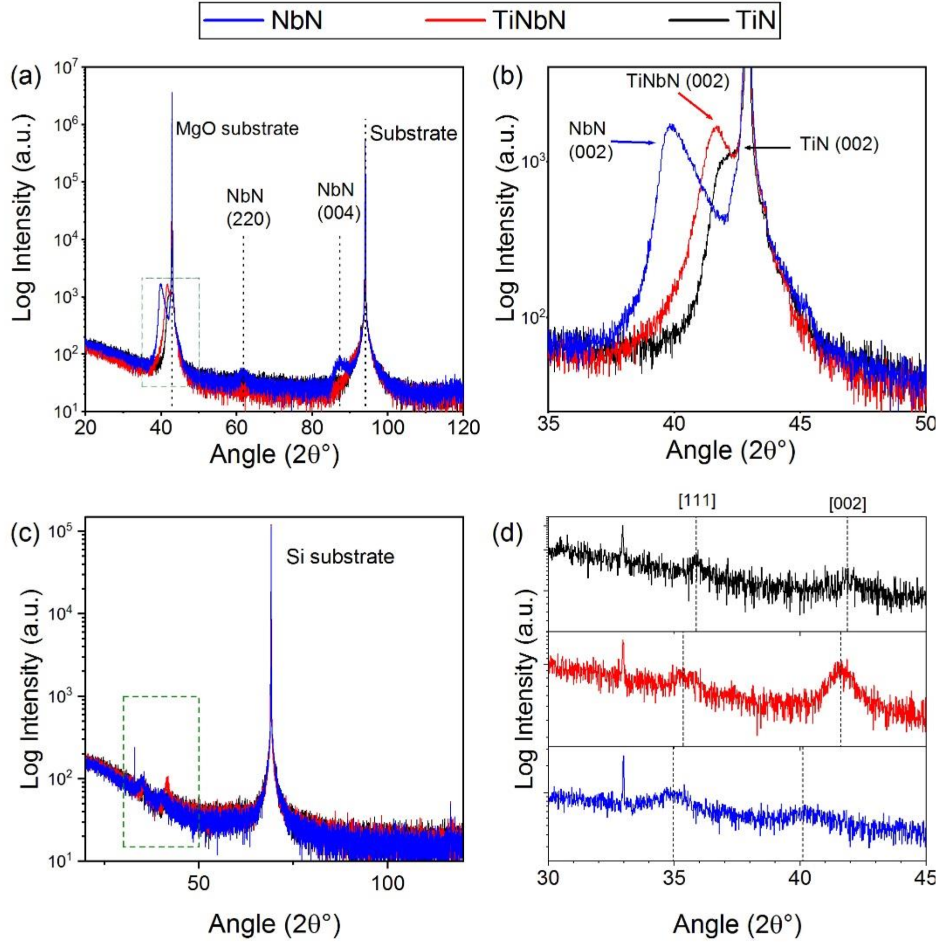

FIGURE 1: (a) Thin film XRD data for TiN, NbN and TiNbNthin films deposited on MgO substrates. (b) Inset displaying (002) peaks for the TMN films, demonstrating the change in lattice parameter. (c) Thin film XRD data for TiN, NbN and TiNbN thin films deposited on Si substrates. (d) Inset displaying [111] and [002] peaks for the TMN films, demonstrating the change in lattice parameter with cation stoichiometry and identity. Dashed lines indicating peak position are included as a guide to the eye.

The unscreened plasma frequency (ω_{pu}) is related to the conduction electron density (N_e) and electron effective mass (m^*) as shown in Equation 1:

$$\omega_{pu} = \sqrt{\frac{e^2 N_e}{\varepsilon_0 m^*}} \qquad (1)$$

The spectral tunability of transition metal nitride films is therefore strongly dependent upon film stoichiometry. Varying the ratio of cations with different numbers of valence electrons allows for the plasma frequency to be tuned, as has previously been reported.[17,23] The ternary films display unscreened plasma frequencies corresponding to wavelengths ranging from 413-420 nm for all substrates, falling between the average epsilon-near-zero values for NbN and TiN of 330nm and 473 nm respectively. When considering the optical properties of the binary and ternary thin films, slight substrate-dependent variation between films is observed, particularly at longer wavelengths. A number of potential reasons exist for this behaviour, with variations in phase, oxygen content and strain all known to contribute to observed optical and dielectric properties.[24,25]

Table 1: Drude broadening term for binary and ternary films deposited on MgO, Si and glass.

Substrate	TiN Γ_D (eV)	TiNbN Γ_D (eV)	NbN Γ_D (eV)
MgO	0.325	0.86	3.6
Si	0.42	0.95	3.2
Glass	0.34	0.92	3.85

As discussed above, XRD data display variations in preferred orientation for films deposited on MgO substrates when compared to films deposited on glass and Si. Films on MgO substrates display increased epitaxy, with [002] preferred orientation. The ellipsometry data shows that MgO films display slightly reduced optical losses compared to those deposited on Si and glass. This is confirmed by analysis of the Drude broadening term (Γ_D) from the DL fitting of the ellipsometry data, summarised in Table 1. A smaller Γ_D term is generally observed for MgO substrates, corresponding to reduced losses. This is likely a result of the increased crystallinity and epitaxy of the films on MgO substrates.

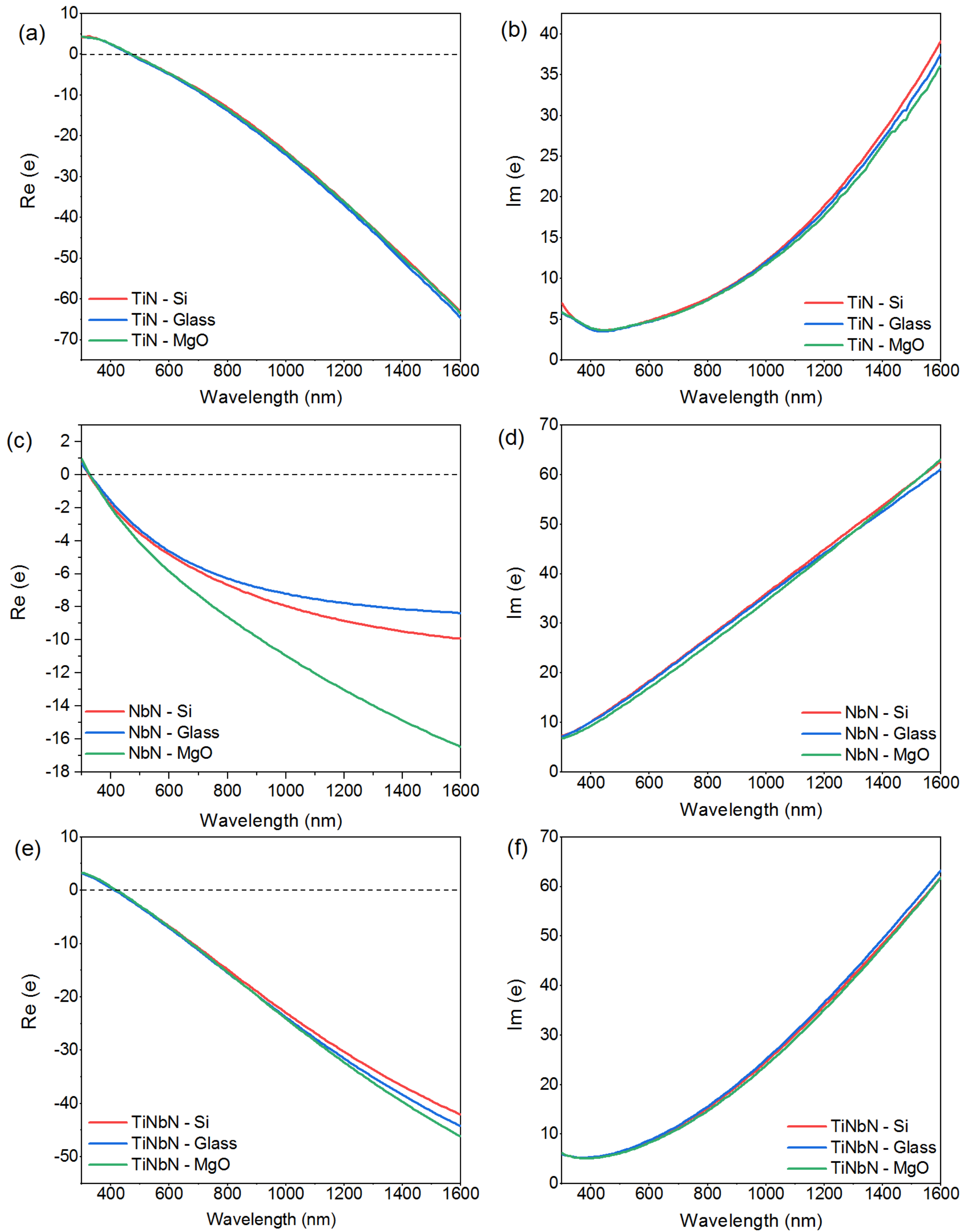

FIGURE 2: Spectroscopic ellipsometry data for TiN (a, b), TiNbN (c, d) and NbN (e, f) thin films deposited on a variety of substrates.

When considering the optical losses of the binary and ternary films, the dielectric contributions, as described by the Lorentz oscillator terms in the DL fit are observed to be located at higher energies and lower wavelengths for NbN, compared to those observed for TiN. The energies for TiN are found to be at visible wavelengths, whereas those of NbN are in the UV, consistent with previous literature.[21] Additionally, the Lorentz oscillators for TiN films have increased strength relative to those fit for NbN films. It should be noted that DL fitting parameters reported in the literature vary significantly, indicative of variations of film quality and also the sensitivity of the ellipsometry fitting procedure. The model fitting parameters detailed in S5 should therefore be considered within this context and regarded as indicative yet not absolute values.

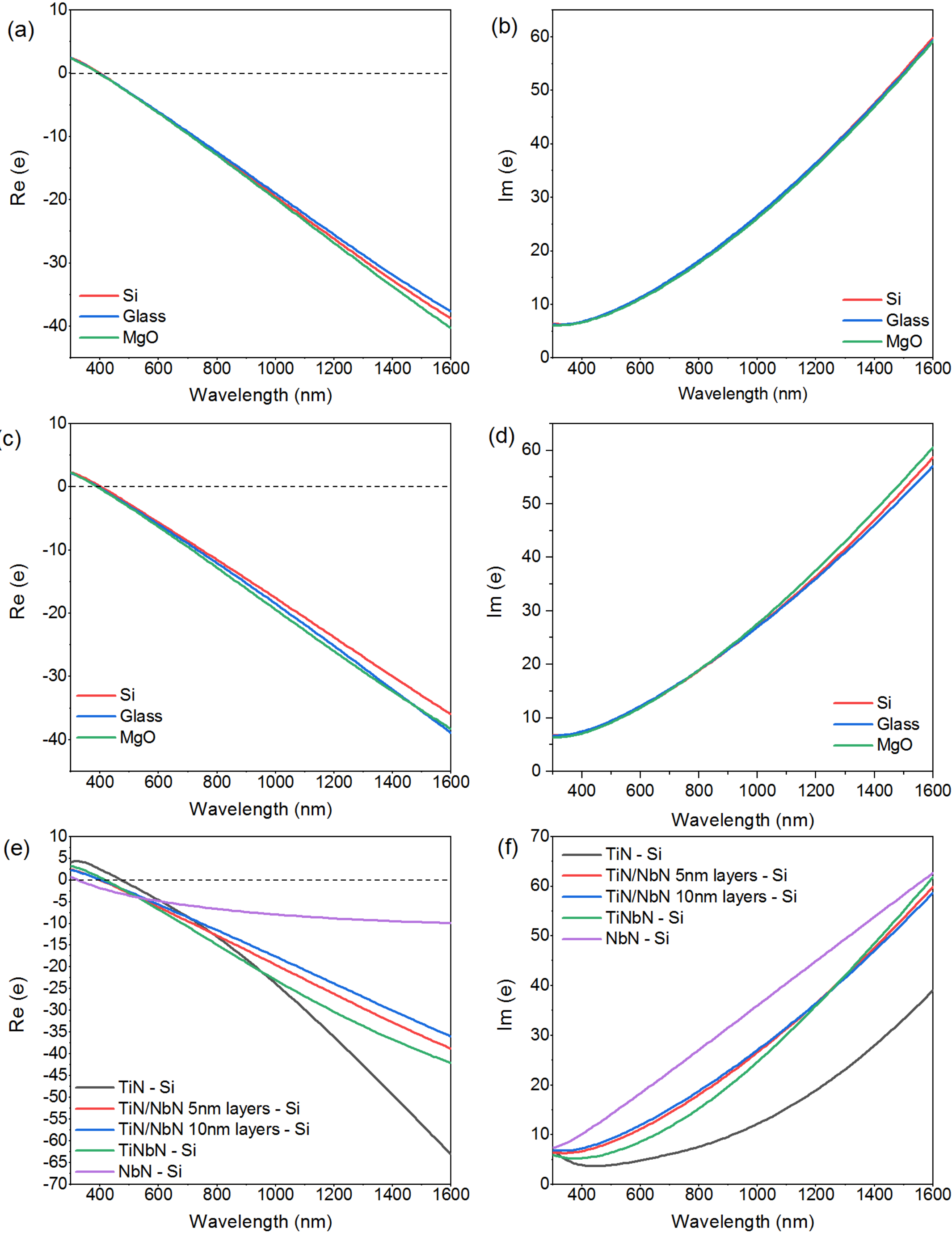

Figure 3: Spectroscopic ellipsometry data for (a,b) 5 nm TiN/NbN layers and (c, d) 10 nm TiN/NbN layers. (e, f) Comparison of ellipsometry data for binary, ternary and layered films on Si substrates. Comparisons of films on other substrates are included in S5.

It has previously been reported for TiN and NbN that phase mixtures and changes in preferred orientation and consequently strain, can result in variations in dielectric permittivity[26,27]. Although there is no significant evidence from the XRD diffraction patterns for the presence of alternative phases (e.g. hexagonal NbN or TiN) it is known that certain phases such as hexagonal δ'-NbN have strong peak overlap with cubic δ-NbN at lower diffraction angles. It is therefore not possible to discount the probability that there are small amounts of alternative phases present. These phases could contribute to the slight variation in the dispersion behaviour observed at longer wavelengths. However, this contribution is likely to be minor, as indicated by the Drude–like behaviour of the binary and ternary thin films.

The presence of small amounts of oxygen impurities and surface roughness of transition metal nitride thin films can also yield distinct differences in the dielectric

permittivity measured. The low-temperature deposition of transition metal nitrides via RF magnetron sputtering has previously been shown to result in the formation of oxynitride thin films due to residual oxygen partial pressures. [25] In order to minimise this effect, residual gas analysis was performed during deposition and showed low levels of contaminants of OH, O and O_2 introduced via the process gas (Figure S1.1). Additionally, a root mean squared roughness of <1 nm indicates that scattering from surface morphological features is unlikely to contribute to variations in dispersion behaviour.

The HIPIMS deposited ternary TMN films are demonstrated to be crystalline and, by minimising the effects of oxygen impurities and surface roughness, HIPIMS is shown to be capable of producing transition metal nitride thin films containing alloyed mixtures of TiN and NbN, with high-quality plasmonic behaviour. The broadband tunability of the ternary TiNbN films indicates the potential for use within optoelectronic devices at a range of functional wavelengths whilst the highly plasmonic behaviour of CMOS compatible films deposited on a variety of substrates suggests the versatility of application that these films can be used for.

Ellipsometric measurements of the layered films also display negative dielectric permittivities and relatively low losses, falling between the higher losses of NbN and that of TiN, similar to the co-sputtered films, as shown in Figure 3. Notably, in contrast to the co-sputtered films, the unscreened plasma frequency of these films is blue-shifted, as shown in Figure 5d. Whilst some variation in plasma frequency may be expected due to minor variations in film stoichiometry and structure in subsequent deposition runs, the difference in ENZ position is significant, approximately 20 nm. However, as previously stated, film stoichiometries for layered and ternary films are comparable, and within error range for equivalent cation stoichiometries for each film. Film stoichiometry therefore does not provide an adequate explanation for the shift in plasma frequency.

A key factor to consider is the strain within the layered films. It has previously been reported that ultrathin layers of films of different composition adopt a single, intermediate lattice parameter for each layer.[28] As a result, the films in each layer are strained, in opposite directions. This is in contrast to co-sputtered films which will adopt a single, pseudo crystalline, unstrained unit cell. XRD diffraction patterns collected for the layered films display broad diffraction peaks, however, a single lattice parameter is indeed observed for the layered structures. As mentioned previously, strain within thin films is known to impact the dielectric properties and vary the refractive index.[24] It is our suggestion that the strain within the layered structures accounts for the shift in plasma frequency when compared to co-sputtered films.

This strain mediated tunability offers an additional degree of freedom when considering device design for plasmonics. It enables access to lower plasma frequencies compared to co-sputtered films and at some spectral ranges displays lower losses, an important factor when considering plasmonic performance. Layered structures also offer the option of depositing a metamaterial with a graded effective refractive index by varying the layer thickness throughout the film. Such control is achievable using HIPIMS.

Sputtering of ultrathin layers often results in the formation of islands within films unless deposited at high temperatures or epitaxially.[29,30] However, the increased peak power density used within the HIPIMS process allows for continuous films with thicknesses less than 10 nm to be deposited. This is a consequence of adatom mobility due to the high fraction of metal ion flux created by the high power used within the HIPIMS process. This allows layers as thin as 5 nm to be deposited. The high ion-to-neutral ratio and presence of metal ions in the HIPIMS process enhances the mobility and contributes to more homogeneous nucleation, dense grain boundaries and larger grains from the outset of the growth.[18]

This is demonstrated by the Scanning Transmission Electron Microscopy micrographs collected for layered NbN/TiN films deposited on Si (Figure 4). Both films display distinct layers of TiN and NbN with well-defined interfacial regions. Slight variation in the film thickness is observed for each layer, as a result of surface roughness during deposition, however, no significant island formation or mixing of layers is observed.

Indeed, the quality of the binary, ternary and layered films is directly a result of the HIPIMS deposition technique used. In comparison with the RF sputtering processes that are characterised with a discharge current density of 0.1 Acm^{-2}, average ion energy of ~40 eV and a ratio of dissociated-to-molecular gas ion flux just below 1,[31] the HIPIMS conditions used in the present study achieved a discharge current density ~0.6 Acm^{-2}, yielding a ratio of dissociated-to-molecular gas ion flux above 1, (Figure S1.2),[18] whilst retaining low average ion energy of 3 eV. The HIPIMS process, therefore, carries a lower risk of ion-induced lattice defects associated with residual stress in the film and thermal damage of the substrate. At the same time, the higher operating voltage of the HIPIMS process of ~500 V ensures higher sputter yields and faster deposition rates compared to RF sputtering where voltages are <300 V. The plasma composition spectroscopic analysis carried out during the deposition, indicated that both gas dissociation (N^{1+} / N_2^{1+}) and metal ionisation (Ti^{1+}/Ti^0) ratios exceed 1, (Figure S1.2). The high flux of atomic nitrogen to the surface promotes the formation of low-mobility TiN clusters and effectively traps Ti on (002) oriented grains. At the same time, metal ions gain energy through the plasma sheath at the substrate surface and become highly mobile adatoms. Finally, the high powers dissipated in the HIPIMS pulse rarefy the gas atmosphere and reduce the energy loss of sputtered atoms on the way to the substrate. These factors work in unison to promote the formation of (002) oriented surfaces. They also lead to the densification of the grain boundaries, smooth the surface and lower the affinity of the coatings towards oxygen.

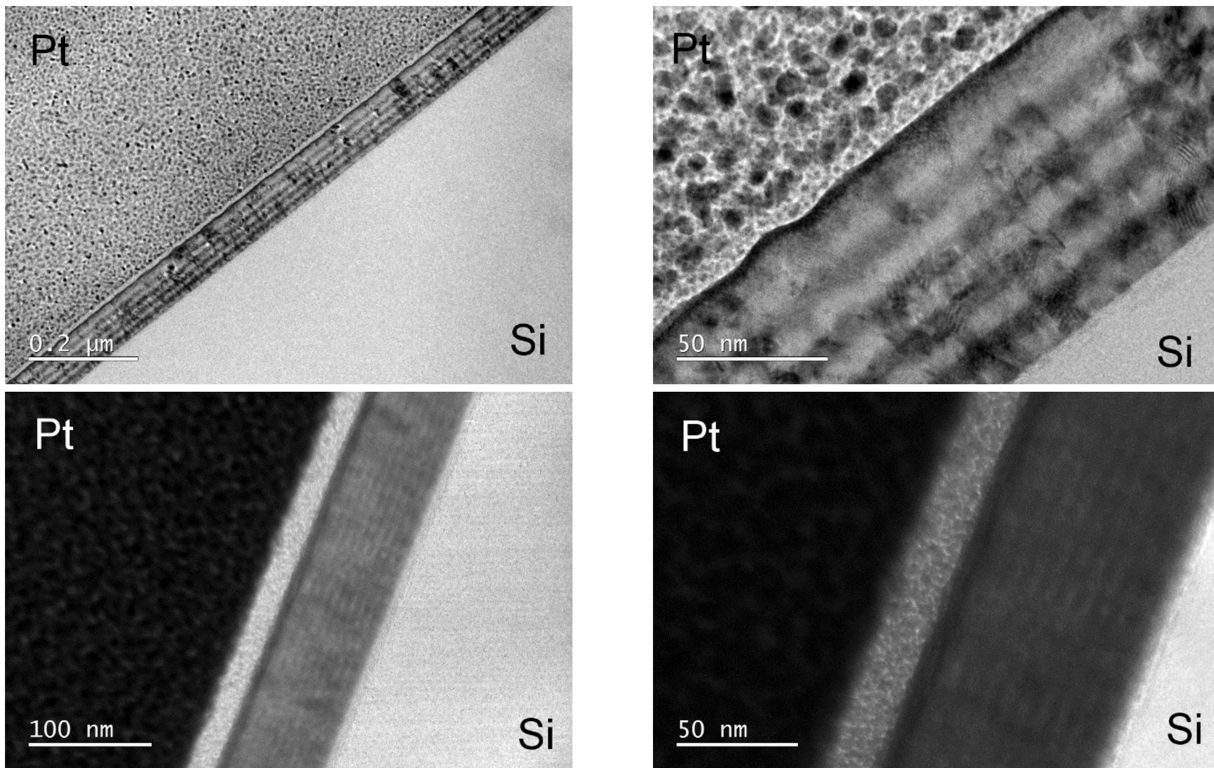

Figure 4: Scanning Transmission Electron Microscopy (STEM) micrographs of layered TiN/NbN samples on Si. TiN layers were first deposited on Si followed by NbN, alternating until the desired total thickness was achieved. Micrographs contain alternating layers of thickness 10 nm (top) and 5 nm (bottom) to a total thickness of 100 nm for both films.

Furthermore, all films were deposited at low, CMOS compatible temperatures (300°C) yet display optical properties comparable to transition metal nitride films deposited at significantly higher temperatures. Figure 5 indicates that the magnitude of the real dielectric permittivity for HIPIMS deposited films is comparable to films deposited via RF magnetron sputtering at 600°C on glass and 850°C on sapphire. Films are also of comparable quality to room temperature TiN films deposited with a shorter substrate-target distance. Notably, TiN films deposited at 300°C using lower HIPIMS peak powers are shown to have a lower magnitude of ε'. It is worth noting here that our HIPIMS films are 100 nm thick, whereas the published data was for films with thickness ~50 nm. However, for metallic films, the penetration depth of incident light is typically less than ~50 nm. Therefore, we believe the comparison between thin films of 100 nm and the literature films of ~50 nm is valid, although the literature films may have additional contributions from substrate reflections in the optical data.

Increasing the peak power density from 3.8 Wcm^{-2} (DC magnetron sputtering) to 76 Wcm^{-2} (HIPIMS) has been shown to increase the magnitude of the real part of the dielectric function (ε').[34] Our observations confirm that further extending the range of power densities to 380 Wcm^{-2} enhances plasma density and nitrogen dissociation, (Figure S1.2), and results in significant improvements in the plasmonic properties of all transition metal nitride thin films reported in this study, as shown in Figure 5 a.

Increased plasma density is also provided as an explanation for high-quality TiN films recently deposited at room temperature via RF magnetron sputtering.[14] These films were deposited with reduced substrate target distance and, as shown in Figure 5, have ε' comparable to films deposited by HIPIMS. However, the ε" values for these films are higher than those obtained in this work, which could be attributed to lattice defects due to the high energy of ion bombardment of tens of eV typical of RF excitation.[31] Indeed, when considering the figure of merit for plasmonic materials (-ε'/ε"), we observe that films deposited by HIPIMS are superior to all but epitaxially grown TiN films deposited at high temperatures (Figure 5c).

CONCLUSIONS

We have deposited high quality, plasmonically active binary and ternary transition metal nitride thin films using High Power Impulse Magnetron Sputtering. The deposition process is CMOS compatible and scalable, allowing the manufacture of plasmonic and optoelectronic devices using transition metal nitrides. The deposition is demonstrated to be possible on a range of industrially relevant substrates and films are spectrally tunable within the wavelength range 325-483 nm.

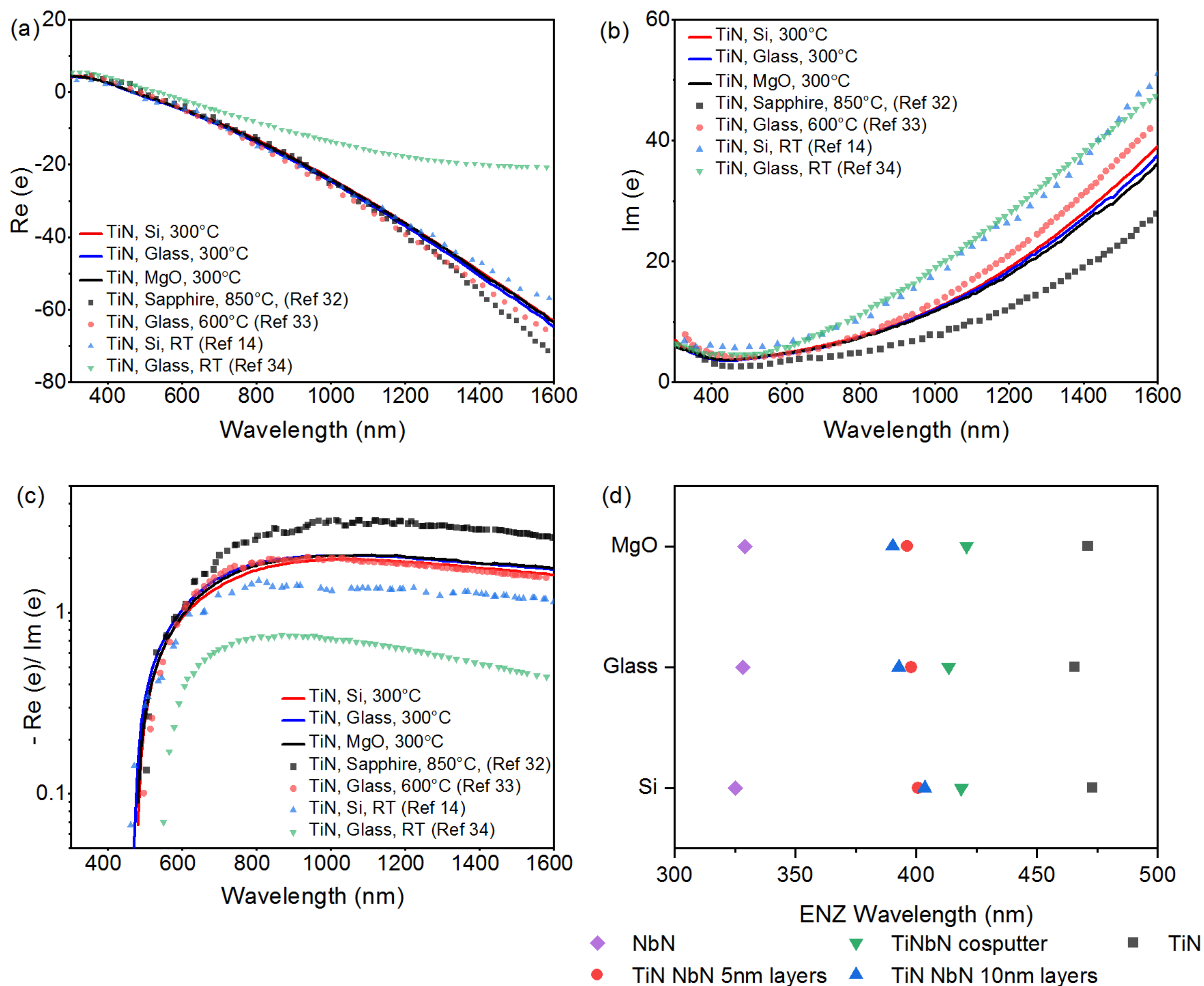

FIGURE 5: Real (a) and imaginary (b) spectroscopic ellipsometry data for TiN films deposited via HIPIMS onto glass and Si substrates. Figures include a comparison to literature values for TiN films.[14,32–34] (c)Figure of merit (-ε'/ε'') (FOM) comparison of TiN thin films and literature data. References 32, 33 and 14 are deposited via RF magnetron sputtering at 850°C, 600°C and RT respectively. Reference 14 has a short substrate target distance of 5 cm. Reference 34 is deposited by HIPIMS with a peak power density of 75W cm^{-2}. All literature films are ~50nm. (d) A comparison of ENZ crossover wavelength for binary, ternary and layered films.

Layered transition metal nitride superlattices are also demonstrated to display high-quality plasmonic behavior. Lattice strain within these films results in a blue-shift of plasma frequency and affords an additional degree of freedom when considering tunability of nitride thin films.

The HIPIMS deposition technique yields high-quality plasmonic films due to the high dissociation and ionization achieved during the deposition process. The increased plasma densities yield high-quality transition metal nitride films even at low temperatures. This method is suitable for the fabrication of plasmonic devices based on metal nitride thin films. Furthermore, the HIPIMS method of deposition used in the current work is scalable to a target length of up to 3 meters and is preferable for large area production, where uniformity of deposition thickness and film properties are critical.

METHODS

Thin films were deposited at the National HIPIMS Technology Centre at Sheffield Hallam University in a CS-400S Cluster system (Von Ardenne Anlagentechnik GmbH) equipped with two confocally-arranged cathodes. Each thin film material was deposited on all substrates types simultaneously. The HIPIMS discharge was operated in a constant current mode using Highpulse 4000 (G2) generators (Trumpf Hüttinger Elektronik sp. z o.o.) at a peak current density of 0.6 A cm^{-2} and peak power density of 380 W cm^{-2}. The constant current mode of regulation of the generator allowed for unprecedented stability and reproducibility during operation of the HIPIMS of TiN discharge with arc rates of ~3 arcs per hour. Residual gas analysis was carried out during the deposition via a differentially-pumped quadrupole mass analyser type Microvision 2 (MKS). Plasma composition analysis was

carried out using a plasma-sampling energy-resolved mass spectrometer type PSM3 (Hiden Analytical Ltd.) whose collection was synchronised with the peak of the pulse delivery at the substrate and also in time-averaged mode. Energy scans were integrated to obtain the total ion flux for each species.

Ellipsometry data was collected using a J. A. Woollam W-VASE ellipsometer. Data were collected over the spectral range 300-1600 nm at incident angles of 65°, 70° and 75°. As the films are optically thick, the experimental data was directly fit using the Marquardt minimisation algorithm to a Drude - Lorentz model, using two Lorentz oscillators. Drude - Lorentz parameters are summarised in S5 Table 1.

XRD data for each film were collected over the $30° \leq 2\theta \leq 50°$ range using a Bruker D2 Phaser X-ray diffraction system operating in the Bragg-Brentano theta-theta geometry with a Cu K_α wavelength of 1.54 Å. Thin film XRD data were collected using a Panalytical Empyrean operating in theta-2theta geometry. The system is equipped with a monochromator and a 2D PIXcel® detector.

Chemical analysis was performed via Energy Dispersive X-ray Spectrometry (EDS) using an Oxford Instruments INCA. Samples were imaged in a Zeiss Leo Gemini 1525 FEG SEM with 10 keV operating voltage and 60 micron aperture. Element quantification was achieved using a titanium standard film, with 97% measurement accuracy. Chemical composition was corroborated using quantitative X-ray fluorescence XRF (Panalytical Epsilon 3 spectrometer) using thin film analysis software (Stratos).

Scanning Transmission Electron Microscopy (STEM) micrographs were collected on a JEOL JEM-2100F TEM with an accelerating voltage of 200 eV. Sample preparation for STEM-EDS analysis was carried out by Focussed Ion Beam (FIB) milling to obtain electron transparent lamellar samples (Helios NanoLab 600 FIB-SEM). Lamellar were coated in a Pt layer to enable the samples to be fixed to the TEM grid.

ASSOCIATED CONTENT

Supporting Information. (S1) Deposition parameter summary and analysis (S2) Stoichiometric analysis (S3) Structural analysis (S4) Film morphology (S5) Ellipsometry fitting summary. "This material is available free of charge via the Internet at http://pubs.acs.org."

AUTHOR INFORMATION

Corresponding Author

*Author to whom correspondence should be addressed: Dr. Peter K. Petrov. E-mail: p.petrov@imperial.ac.uk

Author Contributions

All authors have given approval to the final version of the manuscript.

Funding Sources

This work was partly supported by the Engineering and Physical Sciences Research Council (EPSRC) Reactive Plasmonics Programme (EP/M013812/1) and by the Henry Royce Institute through EPSRC grant EP/R00661X/1.
Ryan Bower acknowledges funding from the EPSRC Centre for Doctoral Training in Advanced Characterisation of Materials (Grant Ref: EP/L015277/1)

REFERENCES

(1) Zhou, N.; Xu, X.; Hammack, A. T.; Stipe, B. C.; Gao, K.; Scholz, W.; Gage, E. C. Plasmonic Near-Field Transducer for Heat-Assisted Magnetic Recording. *Nanophotonics* **2014**, *3* (3), 141–155. https://doi.org/10.1515/nanoph-2014-0001.

(2) Doiron, B.; Mota, M.; Wells, M. P.; Bower, R.; Mihai, A.; Li, Y.; Cohen, L. F.; Alford, N. M. N.; Petrov, P. K.; Oulton, R. F.; Maier, S. A. Quantifying Figures of Merit for Localized Surface Plasmon Resonance Applications: A Materials Survey. *ACS Photonics*. American Chemical Society February 20, 2019, pp 240–259. https://doi.org/10.1021/acsphotonics.8b01369.

(3) Boriskina, S. V.; Ghasemi, H.; Chen, G. Plasmonic Materials for Energy: From Physics to Applications. *Materials Today*. Elsevier October 1, 2013, pp 375–386. https://doi.org/10.1016/j.mattod.2013.09.003.

(4) Fothergill, S. M.; Joyce, C.; Xie, F. Metal Enhanced Fluorescence Biosensing: From Ultra-Violet towards Second near-Infrared Window. *Nanoscale* **2018**, *10* (45), 20914–20929. https://doi.org/10.1039/c8nr06156d.

(5) Wells, M. P.; Bower, R.; Kilmurray, R.; Zou, B.; Mihai, A. P.; Gobalakrichenane, G.; Alford, N. M.; Oulton, R. F. M.; Cohen, L. F.; Maier, S. A.; Zayats, A. V.; Petrov, P. K. Temperature Stability of Thin Film Refractory Plasmonic Materials. *Opt. Express* **2018**, *26* (12), 15726. https://doi.org/10.1364/OE.26.015726.

(6) Graciani, J.; Hamad, S.; Sanz, J. F. Changing the Physical and Chemical Properties of Titanium Oxynitrides TiN 1−x O x by Changing the Composition. https://doi.org/10.1103/PhysRevB.80.184112.

(7) Kassavetis, S.; Bellas, D. V; Abadias, G.; Lidorikis, E.; Patsalas, P. Plasmonic Spectral Tunability of Conductive Ternary Nitrides. *Appl. Phys. Lett.* **2016**, *108* (26), 263110. https://doi.org/10.1063/1.4955032.

(8) Babicheva, V. E.; Kinsey, N.; Naik, G. V; Ferrera, M.; Lavrinenko, A. V; Shalaev, V. M.; Boltasseva, A.; Volkov, S.; Han, Z.; Nielsen, M. G.; Leosson, K.; Keshmiri, H.; Gosciniak, J.; Albrektsen, O.; Bozhevolnyi, S. I. Towards CMOS-Compatible Nanophotonics: Ultra-Compact Modulators Using Alternative Plasmonic Materials. *C)* **2013**, *4* (22). https://doi.org/10.1364/OE.21.027326.

(9) Gosciniak, J.; Atar, F. B.; Corbett, B.; Rasras, M. CMOS-Compatible Titanium Nitride for On-Chip Plasmonic Schottky Photodetectors. *ACS Omega* **2019**, *4* (17), 17223–17229. https://doi.org/10.1021/acsomega.9b01705.

(10) Kim, J. D.; Kim, M.; Chan, C.; Draeger, N.; Coleman, J. J.; Li, X. CMOS-Compatible Catalyst for MacEtch: Titanium Nitride-Assisted Chemical Etching in Vapor Phase for High Aspect Ratio Silicon Nanostructures. *ACS Appl. Mater. Interfaces* **2019**, *11* (30), 27371–27377. https://doi.org/10.1021/acsami.9b00871.

(11) Park, D. G.; Cha, T. H.; Lim, K. Y.; Cho, H. J.; Kim, T. K.; Jang, S. A.; Suh, Y. S.; Misra, V.; Yeo, I. S.; Roh, J. S.; Park, J. W.; Yoon, H. K. Robust Ternary Metal Gate Electrodes for Dual Gate CMOS Devices. *Tech. Dig. Electron Devices Meet.* **2001**, 671–674. https://doi.org/10.1109/IEDM.2001.979597.

(12) Maradudin, A. A.; Sambles, J. R.; Barnes, W. L. *Modern Plasmonics.*; Elsevier Science, 2014.

(13) Jones, S. W. *Diffusion in Silicon*.

(14) Chang, C.-C. C.; Nogan, J.; Yang, Z.-P. P.; Kort-Kamp, W. J. M. M.; Ross, W.; Luk, T. S.; Dalvit, D. A. R. R.; Azad, A. K.; Chen, H.-T. T. Highly Plasmonic Titanium Nitride by Room-Temperature Sputtering. *Sci. Rep.* **2019**, *9* (1).

https://doi.org/10.1038/s41598-019-51236-3.

(15) Sugavaneshwar, R. P.; Ishii, S.; Dao, T. D.; Ohi, A.; Nabatame, T.; Nagao, T. Fabrication of Highly Metallic TiN Films by Pulsed Laser Deposition Method for Plasmonic Applications. *ACS Photonics* **2018**, acsphotonics.7b00942. https://doi.org/10.1021/acsphotonics.7b00942.

(16) Briggs, J. A.; Naik, G. V.; Petach, T. A.; Baum, B. K.; Goldhaber-Gordon, D.; Dionne, J. A. Fully CMOS-Compatible Titanium Nitride Nanoantennas. *Appl. Phys. Lett.* **2016**, *108* (5), 051110. https://doi.org/10.1063/1.4941413.

(17) Del Giudice, L.; Adjam, S.; La Grange, D.; Banakh, O.; Karimi, A.; Sanjinés, R. NbTiN Thin Films Deposited by Hybrid HiPIMS/DC Magnetron Co-Sputtering. *Surf. Coatings Technol.* **2016**, *295*, 99–106. https://doi.org/10.1016/j.surfcoat.2015.10.007.

(18) Ehiasarian, A. P.; Vetushka, A.; Gonzalvo, Y. A.; Sáfrán, G.; Székely, L.; Barna, P. B. Influence of High Power Impulse Magnetron Sputtering Plasma Ionization on the Microstructure of TiN Thin Films. *J. Appl. Phys.* **2011**, *109* (10), 104314. https://doi.org/10.1063/1.3579443.

(19) Wang, Z.; Kawakami, A.; Uzawa, Y.; Komiyama, B. Superconducting Properties and Crystal Structures of Single-Crystal Niobium Nitride Thin Films Deposited at Ambient Substrate Temperature. *J. Appl. Phys.* **1996**, *79* (10), 7837–7842. https://doi.org/10.1063/1.362392.

(20) Patsalas, P.; Kalfagiannis, N.; Kassavetis, S. Optical Properties and Plasmonic Performance of Titanium Nitride. *Materials (Basel).* **2015**, *8* (6), 3128–3154. https://doi.org/10.3390/ma8063128.

(21) Patsalas, P.; Kalfagiannis, N.; Kassavetis, S.; Abadias, G.; Bellas, D. V.; Lekka, C.; Lidorikis, E. Conductive Nitrides: Growth Principles, Optical and Electronic Properties, and Their Perspectives in Photonics and Plasmonics. *Mater. Sci. Eng. R Reports* **2018**, *123*, 1–55. https://doi.org/10.1016/J.MSER.2017.11.001.

(22) Sanjinés, R.; Benkahoul, M.; Sandu, C. S.; Schmid, P. E.; Lévy, F. Electronic States and Physical Properties of Hexagonal β-Nb2N and Δ′-NbN Nitrides. *Thin Solid Films* **2006**, *494* (1–2), 190–195. https://doi.org/10.1016/j.tsf.2005.07.185.

(23) Vasu, K.; Gopikrishnan, G. M.; Ghanashyam Krishna, M.; Padmanabhan, K. A. Optical Reflectance, Dielectric Functions and Phonon-Vibrational Modes of Reactively Sputtered Nb-Substituted TiN Thin Films. *Appl. Phys. A Mater. Sci. Process.* **2012**, *108* (4), 993–1000. https://doi.org/10.1007/s00339-012-7012-5.

(24) Lei, D. Y.; Kéna-Cohen, S.; Zou, B.; Petrov, P. K.; Sonnefraud, Y.; Breeze, J.; Maier, S. A.; Alford, N. M. Spectroscopic Ellipsometry as an Optical Probe of Strain Evolution in Ferroelectric Thin Films. *Opt. Express* **2012**, *20* (4), 4419. https://doi.org/10.1364/OE.20.004419.

(25) Braic, L.; Vasilantonakis, N.; Mihai, A. P.; Villar Garcia, I. J.; Fearn, S.; Zou, B.; Alford, N. M. N.; Doiron, B.; Oulton, R. F.; Maier, S. A.; Zayats, A. V.; Petrov, P. K. Titanium Oxynitride Thin Films with Tunable Double Epsilon-Near-Zero Behavior for Nanophotonic Applications. *ACS Appl. Mater. Interfaces* **2017**, *9* (35), 29857–29862. https://doi.org/10.1021/acsami.7b07660.

(26) Benkahoul, M.; Martinez, E.; Karimi, A.; Sanjines, R.; Le, F. Structural and Mechanical Properties of Sputtered Cubic and Hexagonal NbN Thin Films. *Surf. Coatings Technol.* **2004**, *180* (181), 178–183. https://doi.org/10.1016/j.surfcoat.2003.10.040.

(27) Briggs, J. A.; Naik, G. V.; Zhao, Y.; Petach, T. A.; Sahasrabuddhe, K.; Goldhaber-Gordon, D.; Melosh, N. A.; Dionne, J. A. Temperature-Dependent Optical Properties of Titanium Nitride. *Appl. Phys. Lett.* **2017**, *110* (10), 101901. https://doi.org/10.1063/1.4977840.

(28) Petrov, P. K.; Zou, B.; Wang, Y.; Perkins, J. M.; McComb, D. W.; Alford, N. M. STO/BTO Modulated Superlattice Multilayer Structures with Atomically Sharp Interfaces. *Adv. Mater. Interfaces* **2014**, *1* (3), 1300116. https://doi.org/10.1002/admi.201300116.

(29) Magnus, F.; Ingason, A. S.; Olafsson, S.; Gudmundsson, J. T. Nucleation and Resistivity of Ultrathin TiN Films Grown by High-Power Impulse Magnetron Sputtering. *IEEE Electron Device Lett.* **2012**, *33* (7), 1045–1047. https://doi.org/10.1109/LED.2012.2196018.

(30) Shah, D.; Reddy, H.; Kinsey, N.; Shalaev, V. M.; Boltasseva, A. Optical Properties of Plasmonic Ultrathin TiN Films. *Adv. Opt. Mater.* **2017**, *5* (13), 1700065. https://doi.org/10.1002/adom.201700065.

(31) Ellmer, K.; Cebulla, R.; Wendt, R. Characterization of a Magnetron Sputtering Discharge with Simultaneous RF- and DC-Excitation of the Plasma for the Deposition of Transparent and Conductive ZnO:Al-Films. *Surf. Coatings Technol.* **1998**, *98* (1–3), 1251–1256. https://doi.org/10.1016/S0257-8972(97)00253-3.

(32) Reddy, H.; Guler, U.; Kudyshev, Z.; Kildishev, A. V.; Shalaev, V. M.; Boltasseva, A. Temperature-Dependent Optical Properties of Plasmonic Titanium Nitride Thin Films. *ACS Photonics* **2017**, *4* (6), 1413–1420. https://doi.org/10.1021/acsphotonics.7b00127.

(33) Doiron, B.; Li, Y.; Mihai, A. P.; Cohen, L. F.; Petrov, P. K.; Alford, N. M.; Oulton, R. F.; Maier, S. A. Comparison of the Ultrafast Hot Electron Dynamics of Titanium Nitride and Gold for Plasmonic Applications; 2017. https://doi.org/10.1117/12.2273941.

(34) Yang, Z.-Y.; Chen, Y.-H.; Liao, B.-H.; Chen, K.-P. Room Temperature Fabrication of Titanium Nitride Thin Films as Plasmonic Materials by High-Power Impulse Magnetron Sputtering. *Opt. Mater. Express* **2016**, *6* (2), 540. https://doi.org/10.1364/ome.6.000540.

Table of Contents